

HYBRID ENERGY STORAGE TO INCREASE GRID FLEXIBILITY WHEN CHARGING AN EV FLEET

Edmund SCHAEFER

Saxion UAS/University of Twente– Netherlands
e.w.schaefer@saxion.nl

Gerwin HOOGSTEN

University of Twente - Netherlands
g.hoogsteen@utwente.nl

Johann HURINK

University of Twente – Netherlands
j.l.hurink@utwente.nl

Bart NIJENHUIS

University of Twente - Netherlands
b.nijenhuis-1@utwente.nl

Richard VAN LEEUWEN

Saxion UAS – Netherlands
r.p.vanleeuwen@saxion.nl

ABSTRACT

This paper investigates storage requirements for a grid connected microgrid with PV generation and EV chargers. The aim is to limit the power exchange of the microgrid with the connected main grid. The used power imbalance profiles are constructed using artificially generated EV charging profiles and a PV power production profile. To investigate the storage requirements for this imbalance profile both for hybrid storage and for a single storage device, this imbalance profile is split into multiple sub-profiles. The achieved results show that the required grid connection can be reduced by between 76% and 85% by adding one or more storage device. Additionally, insight is gained into what type of storage devices in a Hybrid Energy Storage System are required with respect to the power, energy and ramp rate of the imbalance profile.

INTRODUCTION

The use of Electrical Vehicles (EVs) is increasing. In this work we consider the EVs to be Battery-Electric Vehicles (BEVs), including automobiles as well as freight lorries and smaller vans such as those used in the parcel distribution sector. This sector currently is increasing the use of EVs in their fleets to meet sustainability goals [1]. For them charging at a central hub with locally generated PV is an intuitive choice, especially when these EVs have planned schedules. However, such a central charging of the EVs may lead to large imbalances and congestion in the local grid and requires additional local grid flexibility or reinforcements.

Grid flexibility can be provided in numerous ways, one of which is through Electrical Storage Systems (ESS). ESSs can manage large power fluctuations at short time intervals and/or shift energy over time. The corresponding systems have technology specific flexibility characteristics and tend to function best at specific timescales [2]. To mitigate the drawbacks of operating an ESS outside of its preferred range, combinations of storage devices, so called Hybrid Energy Storage Systems (HESSs), are potential alternatives. These systems mitigate the drawbacks of the individual ESSs while accentuating the advantages [3].

This simulation study investigates the effects of adding an HESS to a microgrid with an EV fleet, PV generation and a 150kW main grid connection. Hereby, the amount of power required from a main grid should be kept within the limits of the given connection. This means that the maximum amount of power exchange must be reduced to stay within the aforementioned limits. Two scenarios are chosen for investigation, which are assumed to reflect current situations at many distribution centres in the Netherlands.

The contributions of this paper are:

- 1) An examination of HESS sizing requirements for an EV charging microgrid with varying penetrations of PV.
- 2) An examination of the influence of mid-day fast charging an EV fleet in comparison to no mid-day charging on HESS sizing requirements.
- 3) A comparison of HESS and ESS sizing for a microgrid with and EV fleet and PV generation.

METHODS

This section discusses the methods used to investigate HESS sizing of the discussed microgrid. First, EV fleet load profiles and microgrid imbalance profiles are discussed focussing on approaches for HESS sizing through the creation of load profile sub-profiles. Finally, ESS and HESS sizing requirements are examined.

For this analysis we divide the time horizon into discrete time intervals. The creation of an imbalance load profile is done using Equation (1), where $P_{imb}(t)$ is the power imbalance, $P_{PV}(t)$ is the PV generation, which is negative in respect to $P_{imb}(t)$, and $P_{EV}(t)$ is the power demand for charging the EV fleet, all in time interval t .

$$P_{imb}(t) = P_{PV}(t) + P_{EV}(t) \quad (1)$$

EV Fleet Load Profile

In order to generate an EV fleet load profile which reflects the power demand when the fleet is charging, a profile generator tool has been constructed in Python. The model of the generator tool behaves as follows. At any given time

interval, an EV is said to be delivering, charging, or waiting (either waiting to charge if no EV charger is available, or if the time is outside of the defined working hours of the distribution centre). When on delivery, the SoC of the battery depletes according to Equation (2), where $SoC_d(t)$ is the percentage SoC decreases in time interval t , $X_{tr}(t)$ is the distance travelled in time interval t in km and X_{max} is the distance which can be travelled on a full battery charge in km. The values for $X_{tr}(t)$ are calculated by taking the average distance that specific vehicle travels and adding a random amount of noise to ensure that each vehicle will not travel the same distance in each hour.

$$SoC_d(t) = \frac{X_{tr}(t)}{X_{max}} \cdot 100\% \quad (2)$$

When an EV charging station is available, the SoC is increased according to Equation (3), where $SoC_c(t)$ is the percentage the SoC increases in time interval t , $E_{ch}(t)$ is the energy charged in time interval t in kWh and E_{max} is the maximum charge of the EV in kWh. Both $SoC_d(t)$ and $SoC_c(t)$ have to be in the range between 0% (empty) and 100% (full).

$$SoC_c(t) = \frac{E_{ch}(t)}{E_{max}} \cdot 100\% \quad (3)$$

The total power requirement of all chargers is given by Equation (4), where $P_{ct}(t)$ is the average total power required by all chargers at time interval t , $P_c^u(t)$ is the average power requirement of charger u at time interval t and n is the total number of chargers.

$$P_{ct}(t) = \sum_{u=1}^n P_c^u(t) \quad (4)$$

The working hours define the period within which each individual EV depletes. If the charge decreases below a designated discharge safety SoC, the EV is forced to find a charger and charge to a predefined limit. If no charger is available, the EV must wait until one becomes available. Outside of working hours, the SoC of the EVs will no longer decrease, and the EV's will recharge to a 100% SoC. Finally, charging at the distribution centre during defined break hours (where no delivering occurs, for example a lunch break) is possible. For breaks, the EVs are divided into groups, each able to charge for a specific period of time within a given window. After an EV has finished charging, the EV charger cannot be used again for a period in the range of one to two minutes, in order to account for the amount of time it would take to switch vehicles at a charger in real life.

HESS Sizing

Based on given imbalance load profiles, requirements for HESS sizes must be derived, which allow parts of the imbalances to be handled. However, multiple storage types are possible to handle this single load profile, resulting in a large variety of possible combinations of storage sizes. One method for solving this is through load profile decomposition, meaning that the load profile is split into

multiple sub-profiles. Then, each sub-profile can be examined for corresponding HESS requirements. Examples of this approach are given in [4] and [5].

To split the load profile into sub-profiles, signal filtering using low-pass signal filters is applied. Here, frequencies above a cut-off frequency are filtered out, while a specific band remains as a sub-profile. If more than two sub-profiles are required, this process can be repeated by subtracting the created sub-profile from the original sub-profile, choosing a new cut-off frequency which is higher than the one previously used, and repeating the process. To execute this splitting, a tool has been created in Python, the Load Profile Analysis Tool (LPAT).

The tool creates a set of sub-profiles, for which the sum of all sub-profiles is equal to the original profile for all time intervals, see Equation (5). Here, $P_p(t)$ is the original profile in time interval t , $P_p^m(t)$ is the f^{th} sub-profile for time interval t and m is the number of sub-profiles.

$$P_p(t) = \sum_{f=1}^m P_p^f(t) \quad (5)$$

In order to derive storage requirements per sub-profile, the sub-profiles are investigated. Here, requirements are defined as the power, ramp rate and capacity necessary in order to handle a given sub-profile. The maximum and minimum power requirements for a storage are given by the maximum power, P_{max} , and minimum power, P_{min} , of that sub-profile. The minimum and maximum ramp rate values, R_{min} and R_{max} , are found by creating a ramp rate profile. Equation (6) gives the ramp rate R_r for time interval t can be found, where $P_{sub}(t)$ is the power value from the given sub-profile, t is the current time interval, $t-1$ is the previous time interval and T_s is the length of a time interval.

$$R_r(t) = \frac{P_{sub}(t) - P_{sub}(t-1)}{T_s} \quad (6)$$

For the storage capacities, a storage charge/discharge profile is created using (7). Here, $E_p(t)$ is the current energy value and $E_p(t-1)$ the previous energy value. The capacity is then found with Equation (8), where E_{cap} is the capacity, $E_{p,max}$ is the maximum value in the storage profile and $E_{p,min}$ is the minimum value in the storage profile.

$$E_p(t) = E_p(t-1) - P_{imb}(t) \cdot T_s \quad (7)$$

$$E_{cap} = E_{p,max} - E_{p,min} \quad (8)$$

Based on the storage requirements, a choice can be made which storage device is suitable for which part of the total power imbalance (i.e., which sub-profile). If no suitable storage device can be found, a decision can be made to handle the imbalance through other means, for example through the use of a grid connection.

An advantage to using the load profile splitting approach is that it can be used independent of specific storage technologies. No technology specific constraints such as round-trip efficiencies are accounted for. This leads to

more design options when storage technologies are chosen in the future as the design space is not limited too early in the design process.

RESULTS

In the following sections, the results of a simulation study for two scenarios are discussed. First, an analysis is made of possible ESS and HESS sizes in case PV generates the entire energy demand over a year (referred to as 100% PV penetration). In the next step, the PV installation size is varied, and corresponding HESS and ESS capacity requirements are shown.

EV Fleet Charging Scenario I and II

Scenario I considers a situation where no EV charging is possible during working hours and Sunday is not considered as a working day. Scenario II considers a situation where EV fast charging is possible during breaks, and normal EV charging outside of working hours. For Sunday in this second scenario, less deliveries are made, and no charging is possible within working hours. An overview of the two scenarios is given in Table 1. For both scenarios, a maximum grid connection of 150kW (both import and export) is available.

Table 1 Details of EV fleet Scenario I and II

	Scenario I	Scenario II
Number of EVs	40 (Mon – Sat)	40 (Mon – Sat) 10 (Sun)
Number of EV Chargers	40 x 11 kW	40 x 11kW 4 x 150kW (breaks only)
Working Hours		
Weekday	09:00-21:00	09 :00-21:00
Saturday	09:00-17:00	09 :00-17:00
Sunday	None	09 :00-17:00
Breaks	None	Yes, 11:45 – 14:00 (Mon-Sat)

A simulation is executed for an entire year with intervals of 10 seconds in length. This is done to gain a granular enough impression of the behaviour of the model to examine sub-minute behaviour. With this interval length, for standard (11kW) charging we get $E_{ch} = 0.031\text{kWh}$ and for fast (150kW) charging $E_{ch} = 0.417\text{kWh}$. In addition, the vehicles are assumed to be of the type Fiat E-Ducate [6], with a battery size $E_{max} = 47\text{kWh}$. Furthermore, the average travelled distance X_{tr} for each vehicle is assumed to be 12km per hour, and X_{max} is assumed to be 170km.

The scenarios are based on situations that often occurs in the Netherlands, where distribution hubs deliver packages within a relatively small radius, i.e., a city or group of towns. Scenario I leads to a lighter, more predictable pattern of charging and Scenario II results in a more varying pattern of charging (due to the mid-day charging). Figure 1 shows the total charging load profiles of both Scenario I and Scenario II for a week. Figure 2 shows the EV fast charging during breaks from Scenario II.

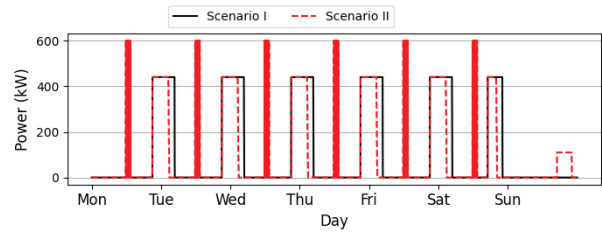


Figure 1 Overall charging profile of the EV fleet for Scenario I and II over one week period

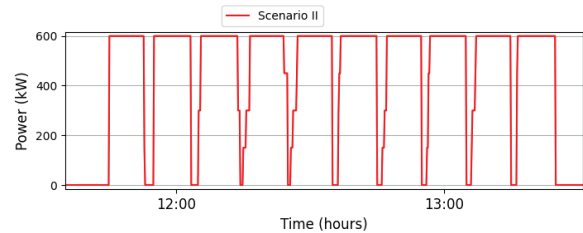


Figure 2 Charging profile of the EV fleet for Scenario II for fast charging in breaks

Storage Sizing, 100% PV Penetration

In order to create an imbalance profile using (1), a PV load profile from April 2020 to March 2021 (one full calendar year) was used. The measurements originate from a site in the Netherlands with a peak power generation of 0.9kW. The profile is then scaled to match the total energy demand of the EV fleet for a year, in this case about 1 GWh for both scenarios. Note that the measured data in August had ten day gap which has been filled by interpolation.

The imbalance profiles are created for both Scenario I and II. LPAT is used to split this original profile into three sub-profiles. For both scenarios, cut-off frequencies of 1/60 Hz (1 minute) and 1/86400 (1 day) are chosen. The reason for this choice is twofold. First, by choosing these frequencies, three sub-profiles are created which represent short-term (sub-minute range), medium-term (minute to day range) and long-term (more than a day range) behaviour respectively. Second, as a grid connection is available in both scenarios, long term behaviour can be handled by this connection. This is economically easier to handle this seasonal behaviour through local storage than by e.g. a hydrogen hub.

Figure 3 and 4 show the sub-profiles created for Scenario I and II respectively. For both figures, P_{dy} represents long-term behaviour, P_{hr} represents medium-term behaviour and P_{rs} represents short term behaviour. For clarity, Figure 5 shows the medium term behaviour P_{hr} for Scenario I over a one month period. In this figure, a day-night cycle is visible, with a deviation on Sunday where no EVs are charging. Figure 6 shows the short term behaviour P_{rs} for Scenario II over a period of twelve hours.

It is evident that the long term behaviour P_{dy} stays within the limitations of the grid connection, which here is

150kW. This sub-profile therefore is suitable to be handled by the connecting grid. Furthermore P_{hr} and P_{rs} appear to have clear charge/discharge patterns, and are therefore suitable for being handled by storage solutions.

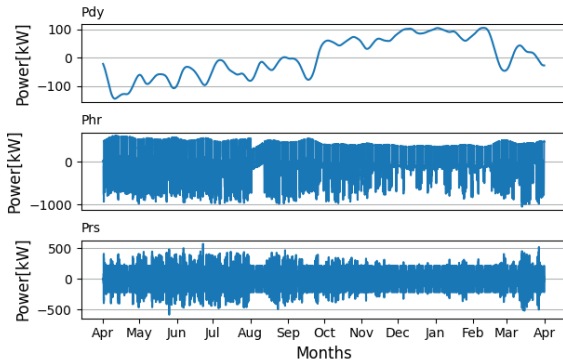


Figure 3 Scenario I Sub-profiles P_{dy} , P_{hr} and P_{rs}

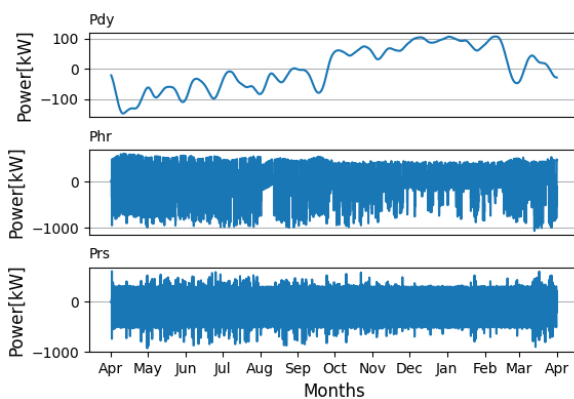


Figure 4 Scenario II Sub-profiles P_{dy} , P_{hr} and P_{rs}

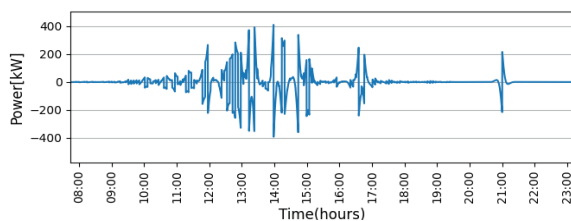


Figure 5 Scenario I P_{hr} , April

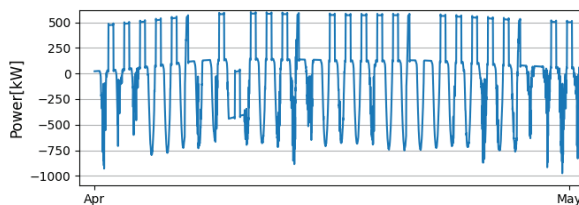


Figure 6 Scenario I P_{rs} , April 1st

In Table 2 the HESS requirements derived from the profiles P_{hr} and P_{rs} are given. Additionally, a joint profile $P_{hr} + P_{rs}$ is created, P_{ss} , in order to gain insight into the storage requirements if a single storage is used. First, it can be noted that the power and ramp-rate values of P_{hr} for both Scenario I and Scenario II are similar, with negligible differences. The exception is the maximum ramp rate

R_{max} , which in Scenario II increases by 18.29%. For P_{rs} , larger differences can be seen for P_{min} and R_{min} , where in Scenario II P_{min} increases by 59.76% and R_{min} by 41.28%. This leads to a conclusion that the fast charging during breaks in Scenario II requires a higher maximum ramp-rate in the medium-term, and higher minimum power and ramp rates in the short-term. With respect to storage capacities, Scenario II requires a 6.7% smaller capacity than Scenario I for P_{hr} , and a 10.41% larger sizing for P_{rs} . In absolute terms there is a 1.13 MWh reduction in the total capacity required in Scenario II compared to Scenario I, and this is a result of less energy having to be stored during the day in Scenario II due to fast charging EVs during break times. The capacities of the storage are 5.5 to 6 times the daily energy demand when averaged out over a week.

Table 2 HESS and ESS sizing for Scenario I and II

	P_{hr} Storage (HESS1)	P_{rs} Storage (HESS2)	P_{ss} Storage (ESS)
Scenario 1			
P_{min} (kW)	-1045.63	-580.30	-1044.27
P_{max} (kW)	600.27	570.50	585.52
R_{min} (kW/s)	-1.86	-94.89	-96.20
R_{max} (kW/s)	1.64	89.86	90.80
Cap (kWh)	16869.14	42.75	16869.42
Scenario 2			
P_{min} (kW)	-1062.72	-927.08	-1061.31
P_{max} (kW)	602.92	612.25	655.37
R_{min} (kW/s)	-1.89	-134.06	-135.05
R_{max} (kW/s)	1.94	91.34	92.30
Cap (kWh)	15739.44	47.2	15739.76

Finally, it is notable that for power and ramp-rate, the requirements for P_{hr} are close to those of P_{ss} , and the ramp-rates of P_{rs} are close to those of P_{ss} . This leads to the conclusion that in the HESS, most of the ramping is covered by P_{rs} and most of the energy shifting is covered by P_{hr} . Hence, it can be concluded that the HESS benefits from using storage devices which are specifically suited to faster ramping or more energy shifting over time.

The balances to be handled by the main grid after storage (improved imbalances) are given in Figure 7 and show a vast reduction in the power required from the grid connection. For Scenario I, P_{max} is reduced by 76% and P_{min} is reduced by 85%. This allows for the use of a

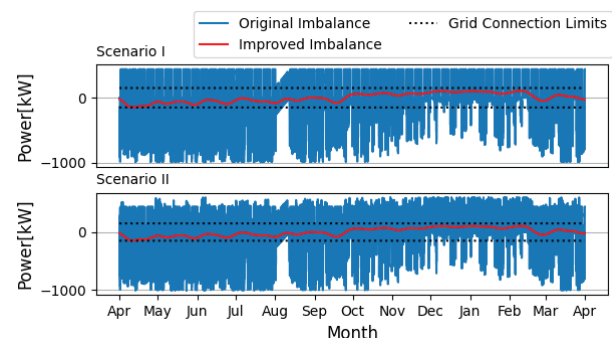


Figure 7 Original and improved imbalance load profiles

smaller grid connection, or may make an upgrade to a larger grid connection superfluous. For Scenario II, the reductions are comparable, 85% for P_{min} and 82% for P_{max} .

Varying PV Penetration

A parameter sweep was conducted for both scenarios, for PV penetrations ranging from 10% to 100% PV in steps of 10%. Here, the main aim is to examine the effect of varying PV energy generation on the HESS sizing. It is worthwhile to note that across all investigated situations, the remaining imbalance to be handled by the connected grid never exceeds the limit of 150kW.

Figure 8 shows the capacity requirements for the medium term profile P_{hr} for various PV penetrations. Here it is evident that Scenario I leads to larger capacities than Scenario II for every penetration. Furthermore both trajectories are parallel and linear from 20% penetration onwards. This is not the case for the capacity requirements for P_{rs} as shown in Figure 9. Scenario I is linear from 30% onward, while Scenario II appears to be linear between 10 and 80%, with a slight bend at 80%. Also, the trajectories are not parallel. In contrast to Figure 8, now all capacities of Scenario II are higher than Scenario I. Again, it is noteworthy that Scenario I requires more medium-term capacity than Scenario II and Scenario II requires more short-term capacity than Scenario I.

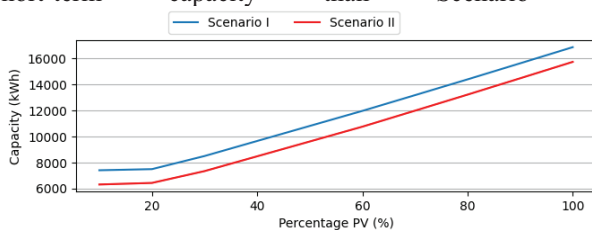


Figure 8 P_{hr} capacity for 10-100% PV penetration.

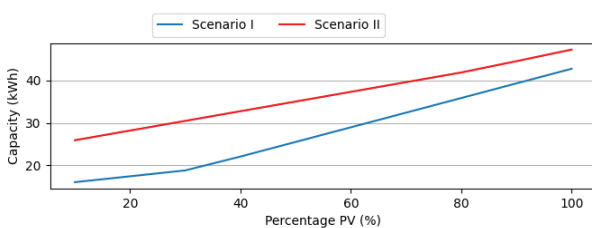


Figure 9 P_{rs} capacity for 10-100% PV penetration

CONCLUSIONS AND OUTLOOK

In this paper an investigation into HESS storage requirements for a microgrid with an EV fleet and varying PV penetrations is presented for two scenarios, one with only evening charging and one with daytime fast charging, in a microgrid with a grid connection of 150kW. It is shown that by adding either an ESS or a HESS, the remaining imbalance to be handled by the connected grid never exceeds 150kW. In comparison to a scenario without storage, the required grid connection can be reduced to between 76% and 85%, which is a considerable improvement. Additionally, when comparing an ESS to a

HESS, it is evident that the majority of the energy shifting is required from a larger storage device operating in a medium-term range, while the power ramping and power export require a smaller storage device operating in a short-term range.

Future research in several directions are worthwhile to be considered. First, it would be advantageous to create an artificial EV Fleet charging profile which is based on more realistic charging and discharging schedules and can be individualized and granular. Next, research is needed into the effects of taking technology specific constraints into account such as round trip efficiency and self-discharge. Finally, the effects of using more or less grid connection power in respect to the required HESS sizing should be investigated.

ACKNOWLEDGMENTS

This work is financially supported by the European Union and the European Fund for Regional Development (Project OP-Oost PROJ-00939).

REFERENCES

- [1] Green Car Congress, "DHL Express purchases 100 Fiat E-Ducato electric vans: 14,000 e-vehicles in delivery fleet across Europe by 2030," 24 April 2021. Available: <https://www.greencarcongress.com/2021/04/20210424-dhl.html>.
- [2] S. Sabihuddin, A. Kiprakis et M. Mueller, "A Numerical and Graphical Review of Energy Storage Technologies," *Energies*, vol. 8, n° 11, pp. 172-216, 2015.
- [3] S. Hajiaghahi, A. Salemnia et M. Hamzeh, "Hybrid energy storage system for microgrids applications: A review," *Journal of Energy Storage*, vol. 21, pp. 543-570, 2019.
- [4] P. Zhao, J. Wang et Y. Dai, "Capacity allocation of a hybrid energy storage systems for power system peak shaving at high wind power penetration level," *Renewable Energy*, vol. 75, pp. 541-549, 2015.
- [5] Y. Liu, W. Du, L. Xiao, H. Wang, S. Bu et J. Cao, "Sizing a Hybrid Energy Storage System for Maintaining Power Balance of an Isolated System With High Penetration of Wind Energy," *IEEE TRANSACTIONS ON POWER SYSTEMS*, vol. 31, 2016.
- [6] Fiat Professional, "E-Ducato," Fiat, [En ligne]. Available: <https://www.fiatprofessional.com/nl/e-ducato-electric/kenmerken>. [Accessed 2021 November 5].